

1 **Exploring the structure of hadronic showers and the**
2 **hadronic energy reconstruction with highly granular**
3 **calorimeters**

4 **Wataru OOTANI^{†,*}**

5 *ICEPP, The University of Tokyo*

6 *7-3-1 Hongo, Bunkyo-ku, Tokyo, Japan*

7 *E-mail: wataru@icepp.s.u-tokyo.ac.jp*

8 Electromagnetic and hadronic calorimeters with an unprecedented high-granularity are being developed by the CALICE collaboration based on a variety of active sensor elements and absorber materials. We present the detailed structures of hadronic showers measured by the CALICE calorimeter prototypes to characterise the different stages of hadronic cascades in the calorimeters as well as comparisons with GEANT4-based simulations using different hadronic physics models. The high granularity of the detectors is exploited in the reconstruction of hadronic energy, both in individual detectors and combined electromagnetic and hadronic systems, making use of software compensation and semi-digital energy reconstruction. The performance of the reconstruction techniques for different electromagnetic and hadronic calorimeters, with silicon, scintillator and gaseous active elements are discussed.

*40th International Conference on High Energy physics - ICHEP2020
July 28 - August 6, 2020
Prague, Czech Republic (virtual meeting)*

[†]on behalf of the CALICE Collaboration

*Speaker

9 1. Introduction

10 An excellent jet energy resolution is required to accomplish the physics goals of future electron-
11 positron colliders. The Particle Flow Approach (PFA) is proposed to achieve an unprecedented jet
12 energy resolution of 3–4 % over a wide energy range[1–3]. High granularity calorimeters required
13 for PFA are under development in the framework of the CALICE collaboration based on various
14 sensor technologies. The concept of the high granularity calorimeters has been validated with
15 full layer prototypes in test beam campaigns. The test beam data provide us not only with the
16 proof-of-principle of the concept but also with a unique opportunity for the detailed studies on
17 the development of the hadronic shower including the validation of the hadronic shower models
18 in GEANT4. The selected results from the test beam data with an emphasis on the studies on the
19 structures of the hadronic showers are presented.

20 2. CALICE Test Beam Prototypes

21 The early CALICE prototypes which were developed for the proof-of-principle of the high-
22 granularity calorimeter concept and extensively tested in beams are summarised as follows.

23 **SiW-ECAL** The “physics prototype” of the SiW-ECAL is based on 30 layers, each of which is
24 composed of a tungsten absorber plate and a sensor layer of $18 \times 18 \text{ cm}^2$ with a matrix of silicon
25 PIN diode of $1 \times 1 \text{ cm}^2$, totalling 9720 cells. The total material depth is $24 X_0$.

26 **ScW-ECAL** The required high granularity is achieved in the ScW-ECAL by scintillator strips
27 aligned alternately in horizontal and vertical orientations. The physics prototype of the ScW-
28 ECAL consists of 30 layers of a tungsten absorber plate and a sensor layer of $180 \times 180 \text{ mm}^2$ with
29 $45 \times 10 \times 3 \text{ mm}^3$ scintillator strips, each of which is read out by a wavelength-shifting fibre coupled
30 to SiPM. The total material depth is $24 X_0$.

31 **AHCAL** The physics prototype of the analogue hadron calorimeter (AHCAL) is composed of 38
32 layers of a steel absorber plate (later tested also with a tungsten absorber) and a layer of scintillator
33 tiles of $30 \times 30 \times 5 \text{ mm}^3$ in the central region and larger tiles in the outer region. Each tile is
34 read out by a wavelength-shifting fibre coupled to SiPM. The active area of the scintillator layer is
35 $90 \times 90 \text{ cm}^2$ with 7608 tiles for the whole prototype. The total material depth amounts to $5.3 \lambda_{\text{int}}$.

36 **DHCAL** The prototype of the digital hadron calorimeter (DHCAL) based on GRPC sensor layer
37 read out by $1 \times 1 \text{ cm}^2$ pad with a 1-bit digital resolution is composed of up to 54 layers of a steel
38 absorber plate (later tested also with a tungsten absorber) and the sensor layer. The transverse size
39 is $96 \times 96 \text{ cm}^2$, and the longitudinal depth corresponds to about $6 \lambda_{\text{int}}$.

40 **SDHCAL** The semi-digital hadron calorimeter (SDHCAL) is also based on GRPC sensor layer
41 read out by $1 \times 1 \text{ cm}^2$ pad, but with a 2-bit digital resolution. The prototype with 48 layers of a steel
42 absorber plate and a $100 \times 100 \text{ cm}^2$ sensor layer has a material depth of about $6 \lambda_{\text{int}}$.

43 3. Hadronic Shower Studies

44 The spatial development of hadronic showers was studied with the test beam data taken at
45 CERN and FNAL by the Fe-AHCAL for positive pions and protons with different initial energies
46 of 10–80 GeV[4]. Fig. 1 shows the longitudinal profiles of showers initiated by (a) pions and

(b) protons of 30 GeV. The shower-start was evaluated on an event-by-event basis with the high longitudinal granularity. The measured profiles are fitted with a two-component function with the parameterisation proposed in Ref.[5]. The profiles are decomposed into “short” and “long” components, and the short component is considered to be the contribution of the electromagnetic component in the hadronic shower. The ratios of the hadronic and electromagnetic response h/e are estimated from the extracted parameters, as shown in Fig. 2 for pions with different initial energies. It shows an only weak energy dependence below 30 GeV and agrees with simulations within 5%.

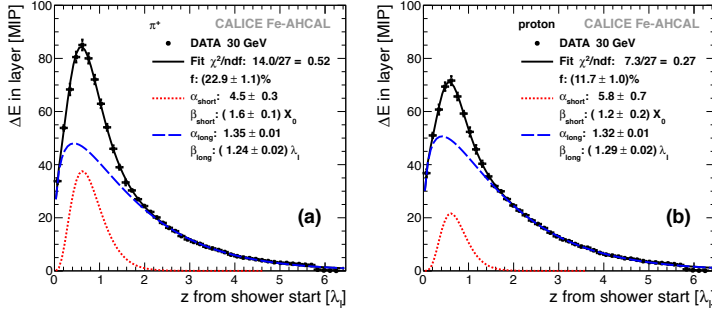


Figure 1: Longitudinal profiles of hadronic showers measured by the AHCAL prototype[4].

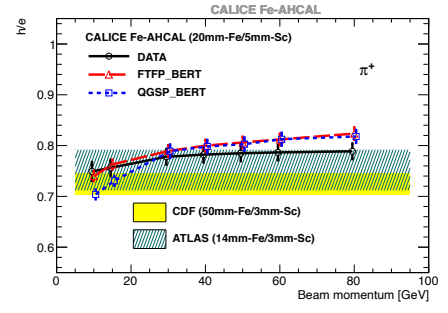


Figure 2: Energy dependence of the h/e estimated by the measured longitudinal profiles[4].

The radial profiles of hadronic showers were studied in more detail with the SDHCAL prototype taking advantage of the finer transverse segmentation[6]. The prototype was exposed to pions at different energies between 5–80 GeV. Fig. 3 shows the radial profiles measured for 20 and 70 GeV pions. The shower barycenter is estimated on an event-by-event basis from the intersection of each layer and the shower axis evaluated by a straight line fit of the unweighted shower hit positions. A smaller width of the profile is observed in the simulation, which is not fully understood.

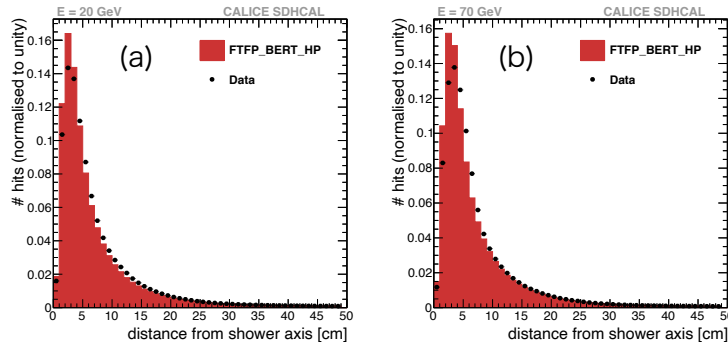


Figure 3: Radial profiles measured with the SDHCAL prototype for (a)20 GeV and (b)70 GeV[6].

The longitudinal profiles of hadronic showers at lower energies were studied with the SiW-ECAL prototype exposed to negative pions of 2–10 GeV at FNAL[7]. Fig. 4(a) shows the measured longitudinal profile for negative pions with an initial energy of 10 GeV. The means of the longitudinal profiles for hit and energy are shown in Fig. 4 (b) and (c), respectively. The measured profiles are in agreement to within 20%, but with a much better agreement for most observables. The longitudinal

65 hit distribution is well described by simulations, while the largest discrepancies are observed in
 66 the longitudinal and radial distributions of the reconstructed energy. It is also observed that the
 67 discrepancies depend on the hadronic shower models in GEANT4.

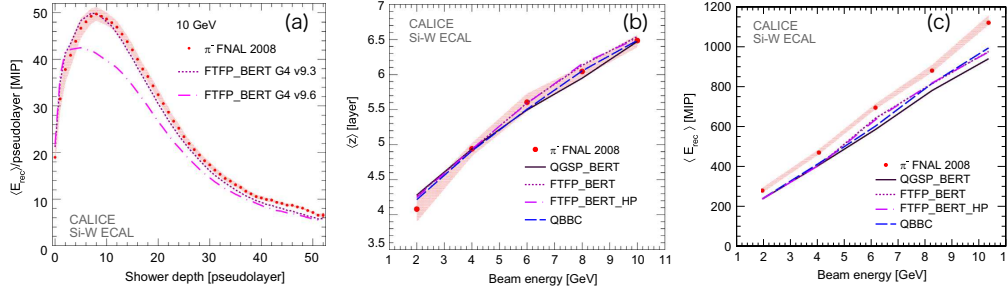


Figure 4: (a) Longitudinal energy profile measured with the SiW-ECAL prototype for negative pions of 10 GeV and the means of the longitudinal hit (b) and energy (c) distributions[7].

68 The high granularity of the CALICE prototypes allows us to study the fine structure of the
 69 hadronic showers using the track segments. Fig. 5(a) shows the typical hadronic shower observed by
 70 the SDHCAL prototype for 50 GeV pions, where the track segments identified by Hough transform
 71 technique are shown in red[8]. The means of the numbers of tracks and the track lengths are shown
 72 in Fig. 5(b) and (c), respectively. They show a reasonably good agreement with the predictions by
 73 simulations, although a slight discrepancy in the number of tracks is seen at high energies. Similar
 74 studies were also done with the AHCAL and SiW-ECAL prototypes[9, 10].

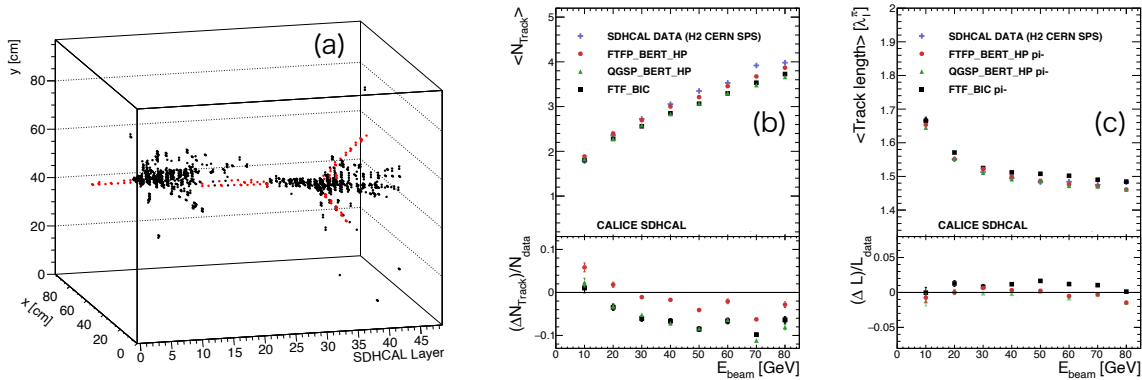


Figure 5: (a) Typical shower observed by the SDHCAL prototype for 50 GeV pion where the track segments identified by Hough transform technique are shown in red; the means of the numbers of tracks (a) and the track lengths (b)[8].

75 4. Hadronic Energy Reconstruction

76 The energy reconstruction for hadronic showers is not trivial due to the complicated processes
 77 for shower development. In particular, the large event-by-event fluctuation of the electromagnetic
 78 and hadronic components in hadronic showers is a crucial limiting factor for non-compensating
 79 calorimeters. A software compensation technique has been applied to the test beam data collected

80 with the combined Sc-ECAL and AHCAL prototypes and Tail Catcher exposed to negative pions
 81 with an energy range of 4–32 GeV at FNAL[11]. The electromagnetic component has a higher
 82 shower density than the hadronic component. The software compensation technique is based
 83 on reweighing individual energy depositions according to the hit energy to compensate for the
 84 difference between the electromagnetic and hadronic response.

85 Fig. 6(a) shows the hit energy spectrum of the AHCAL prototype for 15 GeV pions where the
 86 weights are optimised for each hit energy bin. The hit energy bin weights for each energy bin as
 87 a function of the reconstructed particle energy are shown in Fig. 6(b). Fig. 6(c) shows the energy
 88 resolutions with the standard and the software compensation technique for the combined system
 89 (Sc-ECAL, AHCAL and Tail Catcher). It can be seen that the energy resolutions are significantly
 90 improved by 10–20% with the software compensation technique.

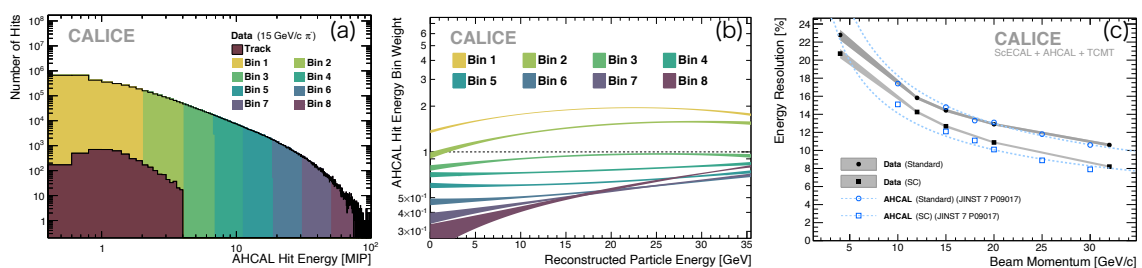


Figure 6: (a) Hit energy spectrum of AHCAL prototype for 15 GeV negative pions[11]. The energy bin weights are optimised for the hit energy bins with different colours. (b) Optimised energy weights for each energy bin as a function of the reconstructed particle energy[11]. (c) Energy resolutions with the standard and the software compensation technique for the combined system (Sc-ECAL, AHCAL and Tail Catcher)[11]. The resolutions only with the AHCAL and Tail Catcher are also shown.

91 The energy reconstruction at the SDHCAL prototype is based on counting the number of
 92 hits but with a multi-threshold readout. The energy is reconstructed as $E = \alpha N_1 + \beta N_2 + \gamma N_3$,
 93 where N_1 , N_2 and N_3 are the exclusive number of hits associated to the first, second and third
 94 thresholds, respectively and α , β and γ are optimised as quadratic functions of the total number of
 95 hits. Fig. 7(a) shows a typical event display for 70 GeV pion. The hits above the third threshold are
 96 concentrated at the shower core and are essentially related to the electromagnetic shower component.
 97 Fig. 7(b) shows the optimised coefficients as a function of the total number of hits. The measured
 98 energy resolutions for pions are shown in Fig. 7(c) where the resolutions with a single threshold
 99 (binary mode) are also shown for comparison. It can be seen that the saturation of the resolution
 100 improvement with the binary mode is mitigated with the multi-threshold mode.

101 5. Summary and Prospects

102 The high granularity calorimeter is a key element to the unprecedented jet energy resolution
 103 with the particle flow calorimetry and is under development based on different sensor technologies
 104 by the CALICE collaboration. Detailed studies on the structures of hadronic showers providing a
 105 validation of the hadronic shower modelling in GEANT4 are carried out with the test beam data
 106 collected by the prototypes of the CALICE high granularity calorimeters. More results are expected

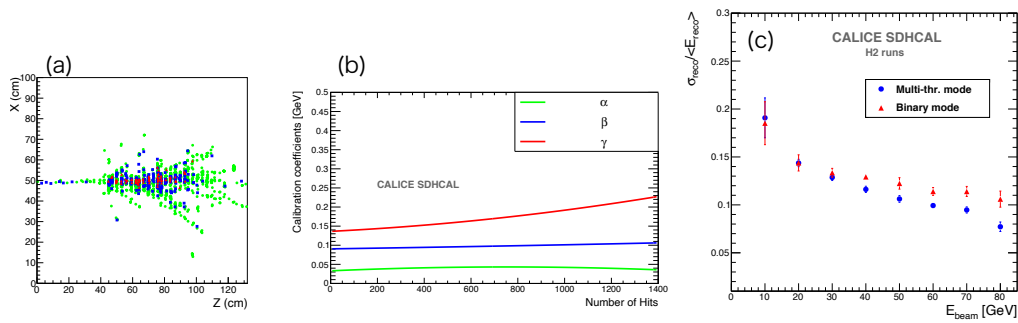


Figure 7: (a) Typical event display for 70 GeV negative pion where the red triangles, the blue squares and the green circles show the hits for the highest, the middle and the lowest thresholds, respectively[12]. (b) Optimised coefficients as a function of the total number of hits[12]. (c) Relative resolutions with the multi-threshold mode where the resolutions with the binary mode is also shown for comparison[12].

107 to come soon from the recent test beam experiments using technological prototypes with improved
 108 performances[13].

109 References

- 110 [1] J.-C. Brient and H. Videau, *eConf C 010630*(2001)E3047 [hep-ex/0202004].
- 111 [2] V.L. Morgunov, *X International Conference on Calorimetry in High Energy Physics*
 112 *(CALOR2002)*, Pasadena, California, U.S.A., 25–29 March 2002.
- 113 [3] M. Thomson, *Nucl. Instrum. Meth. A* **611**(2009)25.
- 114 [4] CALICE collaboration, G. Eigen et al., 2016 *JINST* **11** P06013.
- 115 [5] R.K. Bock, T. Hansl-Kozanecka and T.P. Shah, *Nucl. Instrum. Meth.* **186**(1981) 533.
- 116 [6] CALICE collaboration, Z. Deng et al., 2016 *JINST* **11** P06014.
- 117 [7] CALICE collaboration, B. Bilki et al., *Nucl. Instrum. Meth. A* **794**(2015)240.
- 118 [8] CALICE collaboration, Z. Deng et al., 2017 *JINST* **12** P05009.
- 119 [9] CALICE collaboration, C. Adloff et al., 2013 *JINST* **8** P09001.
- 120 [10] CALICE collaboration, G. Eigen et al., *Nucl. Instrum. Meth. A* **937**(2019)41.
- 121 [11] CALICE collaboration, J. Repond et al., 2018 *JINST* **13** P12022.
- 122 [12] CALICE collaboration, Z. Deng et al., 2016 *JINST* **11** P04001.
- 123 [13] V. Boudry on behalf of CALICE collaboration, *Implementation of large imaging calorimeters,*
 124 *40th International Conference on High Energy physics (ICHEP2020), Jul. 28–Aug.6, 2020,*
 125 *Prague, Czech Republic (virtual meeting).*